Model-Based LOS Path-Following Control of Planar Underwater Snake Robots

Anna M. Kohl, Eleni Kelasidi, Kristin Y. Pettersen, and Jan Tommy Gravdahl

Abstract This chapter presents a model-based control system for straight line path-following of neutrally buoyant underwater snake robots that move with a planar sinusoidal gait in the presence of an unknown, constant and irrotational ocean current. The control system is based on a cascaded design, where a line-of-sight guidance law is employed in the outer control loop in order to provide a heading reference for the robot. In the presence of currents, the guidance scheme is augmented with integral action in order to compensate for the steady state error. This work reviews the theoretical control concept and provides experimental test results with a swimming snake robot that demonstrate the concept of the control system and validate the theoretical analysis.

1 Introduction

Modelling, implementation, and control of underwater snake robots is a growing field in the intersection of biomimetics and marine robotics. Underwater snake robots have emerged from the more established land-based snake robots. Research on land-based snake robots dates back to the 1970s [5] but is still an evolving field of research [13]. A survey of the mechanical design of snake robots can be found in [6]. Another literature review is presented in [14], which focuses additionally on the modelling, analysis, and control of such robots. Underwater snake robots are closely related with robotic fish and are sometimes even considered a special kind

Anna M. Kohl, Eleni Kelasidi, Kristin Y. Pettersen
Centre for Autonomous Marine Operations and Systems (NTNU-AMOS), Department of Engineering Cybernetics, NTNU, Norwegian University of Science and Technology, NO-7491 Trondheim, Norway, e-mail: anna.kohl,eleni.kelasidi,kristin.y.pettersen@itk.ntnu.no

Jan Tommy Gravdahl
Department of Engineering Cybernetics, NTNU, Norwegian University of Science and Technology, NO-7491 Trondheim, Norway e-mail: jan.tommy.gravdahl@itk.ntnu.no

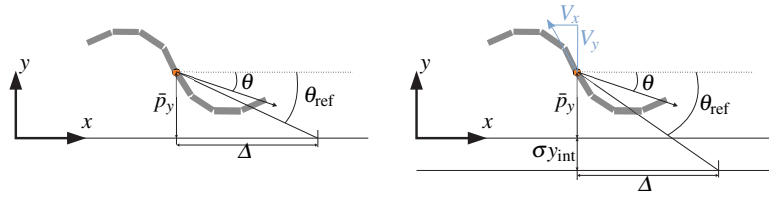

(a) Classical LOS guidance (b) LOS guidance with integral action

Fig. 1 The line-of-sight guidance scheme. The tuning parameters are the look-ahead distance Δ and the integral gain σ.

of fish robots [19]. Surveys on fish inspired robots and their control can be found in [2] and [19].

One important challenge in marine robotics is the development of autonomous control systems for path-following. A strategy for straight line path-following is to apply the well-known line-of-sight (LOS) guidance [3], to determine a reference heading for the control system of the robot. The guidance scheme is visualized in Figure 1(a): the robot steers towards a point on the path that is located at the look-ahead distance Δ in front of the robot along the path. In the presence of ocean currents, this strategy will result in a steady state offset of the path if the currents have a component transverse to the path. This problem can be solved by augmenting the guidance law with integral action, which makes the robot target a point at the look-ahead distance Δ along a displaced path that lies upstream of the desired path, as illustrated in Figure 1(b). A formulation of the integral LOS guidance scheme with a strategy to prevent significant integral windup can be found in [1].

In the context of snake and fish robotics, research on path-following control systems is quite limited. A maneuvering control system for land-based snake robots is proposed in [16] and extended to planar underwater snake robots in [10]. The control system is based on a first-principle model, it considers both velocity and path-following control for generic paths, and is formally shown to be practically stable. A motion planning strategy that is similar to LOS guidance is presented for an eel-like robot in [18]. In [12], trajectory tracking is performed with a fish robot with flow sensors. Another approach is proposed in [4], where a LOS guidance law is employed in order to make a fish-like robot head towards predefined waypoints. The LOS guidance scheme for path-following of snake robots according to Figure 1 has been used both on land and in water. For land-based snake robots, the guidance strategy is investigated in [13] in combination with two different controllers. First, the strategy is implemented in combination with a proportional controller that steers the robot towards the path. Secondly, the heading is controlled with a model-based strategy, which enables an analysis that formally shows stability. For swimming snake robots, the LOS guidance scheme in combination with a proportional heading controller is experimentally investigated in [7]. The augmented integral LOS strategy with the same heading controller is successfully tested in [8]. However, a formal stability analysis of the path-following control system based on this heading

controller is challenging, since a simple proportional controller is combined with a highly non-linear model, and therefore a simulation based Poincaré map analysis is provided instead. The model-based LOS path-following control system that was proposed for land-based snake robots in [13] was recently extended to include integral action and thus be suitable for planar underwater snake robots that are affected by ocean currents in [11], where a formal stability analysis shows uniform semiglobal exponential stability of the control system.

In this chapter we present experimental results with a swimming snake robot for the model-based heading controller in combination with the LOS guidance law without and with integral action. In particular, the experimental results show that the model-based LOS path-following controller for land-based snake robots from [13] also works for swimming robots. Furthermore, the integral LOS path following controller from [11] is experimentally validated. The chapter is structured as follows. Section 2 presents the control-oriented model of an underwater snake robot that has been used for the design of the control systems that are the subject of Sections 3 and 4. The model-based control scheme for snake robots that employs LOS guidance is reviewed and experimentally validated with a swimming snake robot in Section 3. The extension of the model-based control strategy using integral LOS guidance is reviewed in Section 4, where experimental results for this control approach are presented for the first time. Some concluding remarks are made in Section 5.

2 The control-oriented model of the underwater snake robot

The control-oriented model of a snake robot moving in a two-dimensional plane that has been used to design the control systems that are the subject of this work, is based on several simplifying assumptions. To begin with, the robot is assumed to be neutrally buoyant and conduct slow planar motion with a sinusoidal gait such that the angles between adjacent links remain small. For such limited joint angles, the motion of the links with respect to each other can be approximated by linear displacements. It has been shown that the control-oriented model based on these simplifying assumptions captures the behaviour of the robot very well for angles smaller than 30° [13, 9]. The approximation gets gradually less accurate for larger angles, but the qualitative behaviour is still similar.

In essence, the rotational joints of the snake robot are modelled as translational joints, which can be seen in Figure 2. The robot consists of N links of equal length and mass m that are connected by $N-1$ actuated joints. The joint coordinates ϕ_i, $i = 1,\ldots,N-1$ are assembled in the vector $\phi \in \mathbb{R}^{N-1}$. Since the model disregards the rotational motion of the links with respect to each other, they all have the same orientation θ, which also defines the rotation of the robot with respect to the global frame. The robot turns about a virtual point $[\bar{p}_x, \bar{p}_y]^T$ that is located at a distance ε behind its center of mass (CM) at the position $[p_x, p_y]^T$, which is also indicated in Figure 2. The absolute velocity of the robot is defined in the $t-n$ coordinate frame that is aligned with the robot, and thus given by the tangential velocity v_t,

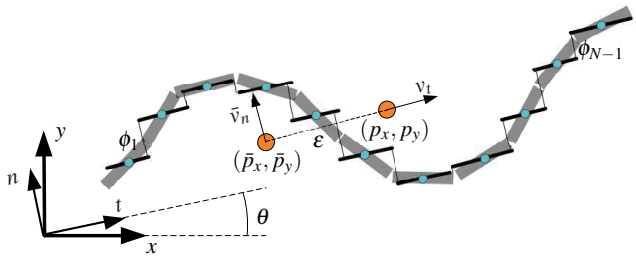

Fig. 2 The control-oriented model of a snake robot is based on approximating the rotational joints by translational joints when the robot conducts a sinusoidal gait.

and the normal velocity $\bar{v}_n$. Since the robot is affected by a current $[V_x, V_y]^T$ in the global coordinate frame, the relative velocities have to be taken into account when modelling the hydrodynamic forces that act on the robot. The relative velocities are given by $v_{t,\text{rel}} = v_t - V_x \cos\theta - V_y \sin\theta$ and $\bar{v}_{n,\text{rel}} = \bar{v}_n + V_x \sin\theta - V_y \cos\theta$. Based on the analysis in [9], the hydrodynamic effects are modelled as linear drag forces, which results in the following model intended for control design:

$$
\begin{aligned}
\dot{\phi} &= \mathbf{v}_\phi, \\
\dot{\theta} &= v_\theta, \\
\dot{\bar{p}}_y &= v_{t,\text{rel}} \sin\theta + \bar{v}_{n,\text{rel}} \cos\theta + V_y, \\
\dot{\mathbf{v}}_\phi &= -\frac{c_n}{m}\mathbf{v}_\phi + \frac{c_p}{m} v_{t,\text{rel}} \mathbf{A}\mathbf{D}^T \phi + \frac{1}{m}\mathbf{D}\mathbf{D}^T \mathbf{u}, \\
\dot{v}_\theta &= -\lambda_1 v_\theta + \frac{\lambda_2}{N-1} v_{t,\text{rel}} \bar{\mathbf{e}}^T \phi, \\
\dot{\bar{v}}_{n,\text{rel}} &= (X + V_x \cos\theta + V_y \sin\theta) v_\theta + Y \bar{v}_{n,\text{rel}}.
\end{aligned}
$$

The joints of the robot are actuated by the control input $\mathbf{u} \in \mathbb{R}^{N-1}$. The parameter c_n is the drag parameter of a single link in the normal direction, c_p is a propulsion coefficient, and λ_1, λ_2 are empirical constants that characterize the turning motion. Furthermore, X and Y are defined as $X = \varepsilon(\frac{c_n}{m} - \lambda_1)$ and $Y = -\frac{c_n}{m}$. The vector operators $\mathbf{A}$, $\mathbf{D}$, and $\bar{\mathbf{e}}$ are defined in [13]. More details on the modelling can be found in [9] and on the transformation to a purely relative velocity representation in [11].

Remark 1. This model does not include the dynamics of the relative forward velocity $v_{t,\text{rel}}$. This is because the purpose of the model is to design a path following control system where the forward velocity is not feedback controlled. Instead, the robot propels itself forward by using a biologically inspired gait, which results in some positive forward velocity $v_{t,\text{rel}} \in [V_{\min}, V_{\max}]$. In the control design process, $v_{t,\text{rel}}$ is therefore treated as a positive model parameter.

3 The model-based control system for LOS path-following

The structure of the relative velocity model presented in Section 2 is the same as that of a land-based snake robot presented in [13]. In fact, if the underwater robot is not exposed to any currents, the relative velocities and the absolute velocities are the same, and the models become identical when replacing the hydrodynamic drag parameters by the ground friction coefficients. It is therefore possible to achieve straight line path-following with a swimming snake robot by using the LOS path-following controller that was presented for land-based snake robots in [13], as long as there is no ocean current.

This section reviews the control system from [13], explains how it was implemented on the amphibious snake robot Mamba, and finally presents an experimental study that validates the conjecture that the control system is also applicable for swimming robots.

3.1 The control system

In the following the model-based LOS path-following control system presented in [13] will be shortly reviewed.

The control objective is to make a snake robot converge to a straight line, align with it, and subsequently travel along it. Without loss of generality, the global coordinate frame is defined such that the path and the global x-axis coincide, and the control objective is formulated as

$$\lim_{t\to\infty} \bar{p}_y(t) = 0, \tag{1}$$

$$\lim_{t\to\infty} \theta(t) = 0. \tag{2}$$

The control problem is solved by a cascaded approach, where the robot achieves a forward velocity with the well known gait lateral undulation, a sinusoidal wave that travels through the snake from head to tail. This way of propulsion is inspired by the motion of biological snakes and can be achieved by controlling each joint i to track the reference signal

$$\phi_{i,\text{ref}} = \alpha \sin(\omega t + (i-1)\delta) + \phi_0, \qquad i = 1,\ldots,N-1. \tag{3}$$

In (3), α is the amplitude of the joint motion, ω is the frequency of the body undulation, δ is the phase shift between adjacent joints, which makes the wave propagate, and ϕ_0 is a constant offset that induces turning motion to the robot. The controller that enforces the reference (3) closes the inner control loop of the cascaded control system and is given by the feedback linearizing control law

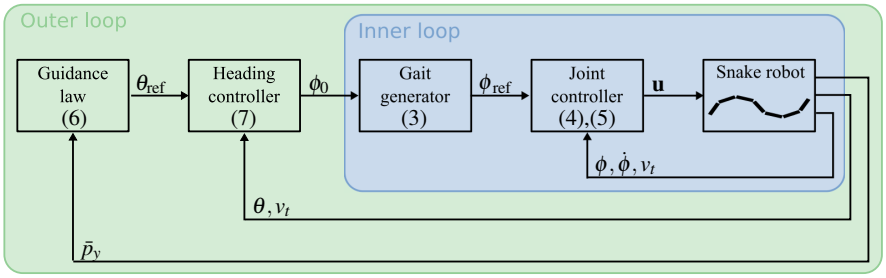

Fig. 3 The structure of the LOS path-following controller for snake robots.

$$\mathbf{u} = m(\mathbf{D}\mathbf{D}^T)^{-1}\left[\bar{\mathbf{u}} + \frac{c_n}{m}\dot{\phi} - \frac{c_p}{m}v_t\mathbf{A}\mathbf{D}^T\phi\right], \tag{4}$$

$$\bar{\mathbf{u}} = \ddot{\phi}_{\text{ref}} + k_{v_\phi}(\dot{\phi}_{\text{ref}} - \dot{\phi}) + k_\phi(\phi_{\text{ref}} - \phi), \tag{5}$$

with the positive control gains k_ϕ and k_{v_ϕ}. It was proven in [13] that this control law exponentially stabilizes the joint coordinate errors $\tilde{\phi}_i = \phi_i - \phi_{i,\text{ref}}$ to zero. After closing the inner control loop according to the above equations, ϕ_0 can be interpreted as a new control input that induces turning motion to the inner cascade.

In the outer control loop, the robot is steered towards the path and thus forced to fulfil the control objectives (1),(2) by enforcing the heading reference

$$\theta_{\text{ref}} = -\arctan\left(\frac{\tilde{p}_y}{\Delta}\right) \tag{6}$$

given by the LOS guidance law. It was shown in [13] that the heading controller

$$\phi_0 = \frac{1}{\lambda_2 v_t}\left[\ddot{\theta}_{\text{ref}} + \lambda_1\dot{\theta}_{\text{ref}} - k_\theta(\theta - \theta_{\text{ref}})\right] - \frac{1}{N-1}\sum_{i=1}^{N-1}\alpha\sin\left(\omega t + (i-1)\delta\right) \tag{7}$$

with the positive control gain k_θ makes the equilibrium of the heading error $\tilde{\theta} = \theta - \theta_{\text{ref}} = 0$ uniformly globally exponentially stable.

The structure of the control system is summarized in the block diagram in Figure 3. In [13], the control system was proven to κ-exponentially stabilize the error dynamics to zero, corresponding to satisfying the control objectives (1),(2) under the assumption that the robot moves at a velocity $v_t \in [V_{\min}, V_{\max}]$ and the following sufficient condition:

Theorem 1 (see Theorem 8.2 in [13]). *If the look-ahead distance Δ of the LOS guidance law (6) is chosen such that*

$$\Delta > \frac{|X|}{|Y|}\left(1 + \frac{V_{\max}}{V_{\min}}\right), \tag{8}$$

the control objectives (1),(2) are enforced by the path-following control system in Figure 3.

Remark 2. The model-based heading controller (7) has to be implemented with care in order to avoid singularity issues when the forward velocity of the robot is zero, $v_t = 0$. Since the robot gains a positive forward velocity by moving with a sinusoidal gait, this issue will only occur when starting up the system and can be avoided by adding a saturation function to ϕ_0 or setting the control input ϕ_0 to zero if the forward velocity $v_t = 0$ is smaller than a certain bound.

3.2 Implementation of the control system

The control system presented in Section 3.1 was implemented on a laptop that runs LabVIEW 2013. The proportional controllers that are implemented in the microcontrollers of each joint of the test robot replaced the low level control law (4),(5), because the theoretical feedback linearizing control law (4) requires torque control while the joints of the test robot are position controlled. This does not invalidate the theoretical control structure, because the cascaded analysis just requires that the joint error dynamics are exponentially stabilized, regardless which controller is used. The control input ϕ_0, which is used to induce turning motion, is a linear displacement in the control-oriented model. However, since it has been shown previously [13, 9] that the control-oriented model presented in Section 2 still captures the qualitative behaviour of the robot with its revolute joints, (7) was implemented as the heading controller. The model parameters of the control-oriented model λ_1 and λ_2 that show up in the heading controller (7) were treated as control gains analogously to the implementation in [13], where the control system was tested with a land-based snake robot. In order to implement the heading controller (7), the forward velocity v_t needed to be approximated from the data of an external motion capture system. It was estimated as the displacement of the CM divided by a sampling interval of 2 s. In order to obtain smooth time derivatives of the heading reference θ_{ref}, the commanded angle θ_{ref} was passed through a 3rd-order low-pass filtering reference model. The parameters of the reference model were $T = \frac{1}{2\pi}$ and $\zeta = 1$. Details on the reference model can be found in [13]. Finally, in order to avoid the singularity in (7) or self-collision of the physical robot, the heading control input ϕ_0 was saturated at $\phi_{0,\max} = \pm 20^\circ$, and filtered with a first-order low-pass filter with the cut-off frequency 1.25 Hz. Since the exact model parameters that are required for calculating the offset ε are unknown, it was assumed that the robot turns about its CM, i. e. the parameter was set to $\varepsilon = 0$. In order to close the feedback control loop, reflective markers were attached to the robot tail, and the angle and position measurements of these markers were obtained from an external motion capture system. On the second laptop, both Qualisys Track Manager (QTM) and Labview 2013 were installed and

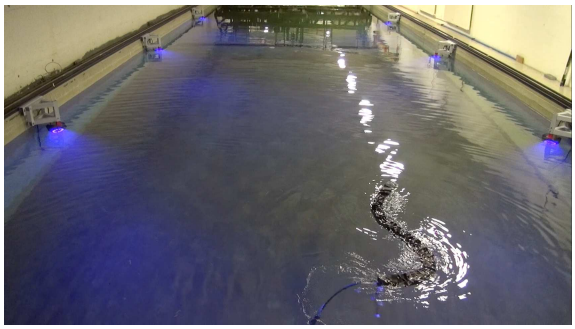

Fig. 4 The snake robot Mamba in the MC-lab. The cameras of the motion capture system are mounted on both sides of the tank.

communicated with each other. The obtained position data were sent from the second laptop in Labview 2013 via UDP in real-time at a sample frequency of 10 Hz. The angles of each single link and the position of the CM p_x, p_y were then obtained from the angle and position measurements of the reflective markers in combination with the single joint angles, analogously to the implementation in [7]. The orientation of the robot was estimated by the average of the link angles, $\bar{\theta}$. The control

Table 1 The control gains of the LOS path-following control system

α	ω	δ	k_θ	λ_1	λ_2	Δ
30°	90°	40°	0.4	0.5	0.2	1.8 m

gains of the system were tuned according to Table 1. Since neither the exact parameters of the control-oriented model in Section 2 were known, nor did we know the velocity of the robot in advance, it was difficult to find a numeric value for the lower bound on the look-ahead distance Δ according to (8). Consequently, we interpreted this condition as the requirement to choose Δ sufficiently large.

3.3 Experimental validation of the control system

The LOS path-following control system that was reviewed in Section 3.1 was experimentally tested in the Marine cybernetics laboratory (MC-lab) at NTNU [17]. The MC-lab is a small wave basin that is suitable for the testing of marine control systems. The tank dimensions are 40 m in length, 6.45 m in width, and 1.5 m in depth. For our tests, the wave maker was deactivated. In order to obtain accurate position measurements for the control system, six cameras of the underwater motion capture system Qualisys [21] were mounted on the walls of the basin, three on each side. The snake robot Mamba [15] was used to test the LOS control system. Figure 4 shows the robot in the MC-lab. Mamba is a modular snake robot that was designed and built at NTNU and is suitable for operations both on land and in wa-

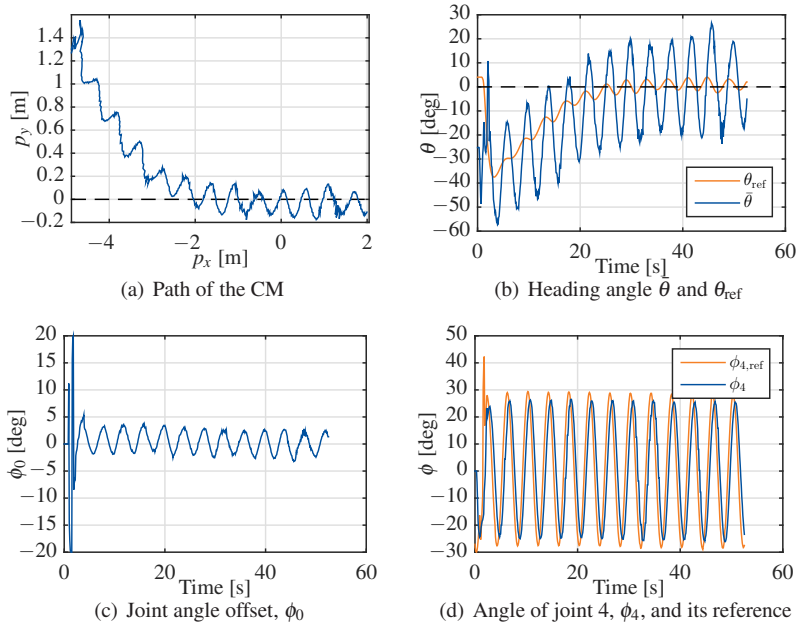

(a) Path of the CM

(b) Heading angle θ and θ_{ref}

(c) Joint angle offset, ϕ_0

(d) Angle of joint 4, ϕ_4, and its reference

Fig. 5 Experimental results of the first scenario: Model-based LOS path-following with the robot initially headed towards the path.

ter. It consists of nine horizontal joints and nine vertical joints and is connected to a power source and communication unit with a slender positively buoyant cable. During all our tests an angle of zero was enforced on the vertical joints in order to test the two-dimensional control scheme. The robot joints are waterproof down to 5 m and equipped with a servo motor, a microcontroller card, and several sensors. The joint angles are controlled by a proportional controller, which is implemented on the microcontroller card that communicates over a CAN bus. More details about the physical robot can be found in [15]. For our tests, reflective markers for the Qualisys motion capture system were attached to the tail of the robot and the robot was put into a synthetic skin for additional waterproofing. Detailed information about the skin is provided in [7]. The amount of air that is contained inside the skin can be varied manually by a pneumatic valve, which changes the buoyancy of the robot. For the two dimensional control system that was tested, a slightly positive buoyancy was enforced in order to make the robot stay close to the surface and thus not require depth control. The control system from Section 3.1 was successfully tested in two different scenarios. In the first case, the robot was initially headed towards the path, and in the second case it was initially headed approximately parallel to the path. In both cases, the robot was initially straight and kept in a fixed position.

The results of the different test scenarios are presented in Figures 5 and 6. The path of the CM of the robot is plotted in Figures 5(a) and 6(a). It can be seen that the robot approached the path and stayed on it. In steady state, the CM did not stay constantly on the path, but oscillated about it. This is a consequence of the oscillating

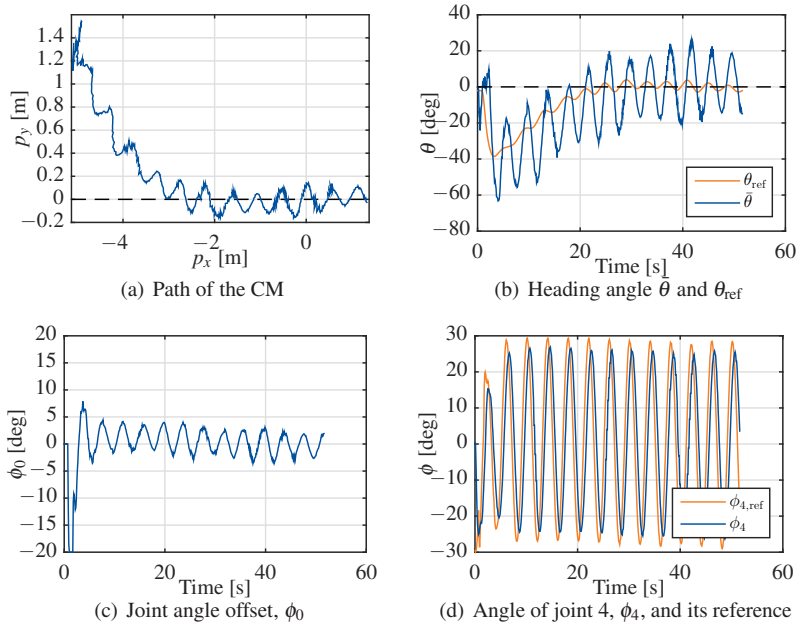

(a) Path of the CM
(b) Heading angle $\bar{\theta}$ and θ_{ref}
(c) Joint angle offset, ϕ_0
(d) Angle of joint 4, ϕ_4, and its reference

Fig. 6 Experimental results of the second scenario: Model-based LOS path-following with the robot initially headed parallel to the path.

nature of snake locomotion and an effect that is not captured by the control-oriented model, where the rotational motion of the links is disregarded. The same applies to the heading of the robot, $\bar{\theta}$, as can be observed in Figures 5(b) and 6(b). Instead of converging to zero, the measured signal kept oscillating about zero as a consequence of the simplifications in the control-oriented model. However, after reaching the reference, the measured signal clearly stayed as close as the oscillating motion allowed. The reference signal θ_{ref} itself kept oscillating about zero as a consequence of the deviations of the CM from the path. The control input for turning motion, ϕ_0, is displayed in Figures 5(c) and 6(c). In the first seconds, before the robot had reached sufficient forward velocity, the signal was saturated. After the robot had reached the path on the other hand, ϕ_0 was oscillating about zero, thus allowing the robot to follow the oscillating heading reference θ_{ref}. Finally, the reference signal and the measured signal of the arbitrarily chosen joint number four is shown in Figures 5(d) and 6(d). It is obvious that the joints were tracking their references.

It can be concluded from the experimental results that the model-based LOS path-following controller works for swimming snake robots without any modification, despite the simplifications in the control-oriented model. The control objectives (1),(2) are approximately satisfied. The remaining oscillations after convergence are an inherent element of snake robots conducting sinusoidal gaits, and they are not captured by the control-oriented model, which explains why they are not cancelled by the model-based control approach.

4 The model-based control system for integral LOS path-following

The LOS path-following controller for snake robots, which was reviewed and tested in the previous section, works for underwater snake robots only under the condition that there are no ocean currents acting on the robot. In the presence of currents, the LOS guidance law will not enable the robot to converge to and stay on the path, so a different guidance law has to be employed. In addition, the model of the robot is a different one, since the current effect has to be accounted for in the model and the hydrodynamic forces that act on the robot now no longer depend on the absolute velocities, but rather on the relative velocities. In this section, the model-based integral LOS path-following control system that was presented in [11] will therefore be used for snake robot control in the presence of ocean currents. At first, the control system will be reviewed, secondly, the implementation of the control laws on the physical robot will be discussed, and finally an experimental validation of the control system will be presented.

4.1 The control system

In the following the model-based integral LOS path-following control system presented in [11] will be shortly reviewed.

The control objective is to make an underwater snake robot converge to a straight line, and subsequently travel along it at some heading θ^{eq}. Without loss of generality, the global coordinate frame is defined such that the path and the global x-axis coincide and the control objective is formulated as

$$\lim_{t\to\infty} \bar{p}_y(t) = 0, \tag{9}$$

$$\lim_{t\to\infty} \theta(t) = \theta^{\text{eq}}. \tag{10}$$

The steady-state heading θ^{eq} is in general non-zero, and is a crab angle that enables the robot to compensate for the sideways component of the current. Its value depends on the speed of the robot and the magnitude of the ocean current.

The structure of the control system is the same as of the LOS path-following controller in Section 3.1 and visualized in the block diagram in Figure 7. The reference for the joint controller in the inner control loop is augmented to the more general

$$\phi_{i,\text{ref}} = \alpha g(i) \sin(\omega t + (i-1)\delta) + \phi_0, \qquad i = 1,\ldots,N-1, \tag{11}$$

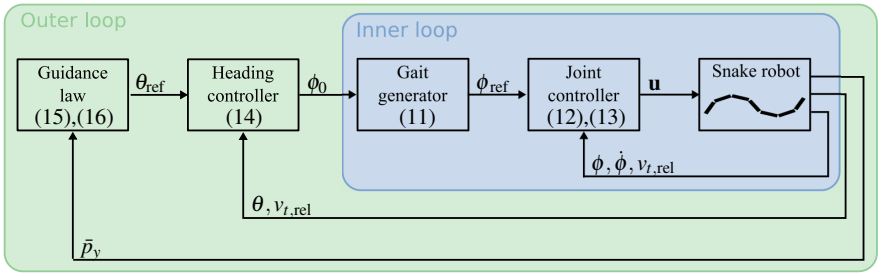

Fig. 7 The structure of the integral LOS path-following controller for snake robots.

where the amplitude of the undulation can be varied along the body with the scaling function $g(i)$. For instance, choosing $g(i) = \frac{N-i}{N+1}$ will mimic the swimming motion of eels [7]. The feedback linearizing joint controller and the heading controller in the outer control loop are based on the complete underwater model in Section 2, which takes the relative velocity into account, and the new gait reference (11). They read as

$$\mathbf{u} = m(\mathbf{D}\mathbf{D}^T)^{-1}\left[\bar{\mathbf{u}} + \frac{c_n}{m}\dot{\phi} - \frac{c_p}{m}v_{t,\text{rel}}\mathbf{A}\mathbf{D}^T\phi\right], \tag{12}$$

$$\bar{\mathbf{u}} = \ddot{\phi}_{\text{ref}} + k_{v_\phi}(\dot{\phi}_{\text{ref}} - \dot{\phi}) + k_\phi(\phi_{\text{ref}} - \phi) \tag{13}$$

and

$$\phi_0 = \frac{1}{\lambda_2 v_{t,\text{rel}}}\left[\ddot{\theta}_{\text{ref}} + \lambda_1\dot{\theta}_{\text{ref}} - k_\theta(\theta - \theta_{\text{ref}})\right] - \frac{1}{N-1}\sum_{i=1}^{N-1}\alpha g(i)\sin\left(\omega t + (i-1)\delta\right). \tag{14}$$

The guidance law in the outer loop controller needs to be changed in order to account for the ocean current. Instead of the LOS guidance in Section 3.1, the augmented integral LOS guidance scheme is employed now:

$$\theta_{\text{ref}} = -\arctan\left(\frac{\bar{p}_y + \sigma y_{\text{int}}}{\Delta}\right), \tag{15}$$

$$\dot{y}_{\text{int}} = \frac{\Delta\bar{p}_y}{(\bar{p}_y + \sigma y_{\text{int}})^2 + \Delta^2}. \tag{16}$$

The integral action in (16) enables the robot to compensate for the steady-state error that would result from applying the LOS guidance in Section 3.1 in the presence of ocean currents. Due to the integral action, when $\bar{p}_y$ converges to zero, the reference angle will converge to a non-zero crab angle θ^{eq}, which is necessary to counteract currents that are transverse to the path.

In [11], the control system in Figure 7 was transformed into error coordinates that form a cascaded system. The assumption was made that the robot moves at a

relative velocity $v_{t,\mathrm{rel}} \in [V_{\min}, V_{\max}]$ that is large enough to counteract the current. Furthermore, the ocean current was assumed to be constant, irrotational, and of a magnitude smaller than the bound $V_{c,\max}$. It was shown in [11] that the origin of the system is uniformly semi-globally exponentially stable under the following sufficient condition:

Theorem 2 (see Theorem 2 in [11]). *If the look-ahead distance Δ and the integral gain σ of the integral LOS guidance law (15),(16) are chosen such that*

$$\Delta > \frac{|X| + 2V_{c,\max}}{|Y|}\left[\frac{5}{4}\frac{V_{\max} + V_{c,\max} + \sigma}{V_{\min} - V_{c,\max} - \sigma} + 1\right], \tag{17}$$

$$0 < \sigma < V_{\min} - V_{c,\max}, \tag{18}$$

the control objectives (9),(10) are enforced by the path-following control system in Figure 7, and the steady state heading is

$$\theta^{\mathrm{eq}} = -\arctan\left(\frac{V_y}{\sqrt{v_{t,\mathrm{rel}}^2 - V_y^2}}\right). \tag{19}$$

Remark 3. For implementing the heading controller (14) on a robotic system, measurements of the relative velocity are needed. In addition, the first two derivatives of the heading reference θ_{ref} are required. These depend on the absolute velocity of the robot, but for a practical system it is much preferred to obtain them by passing the reference signal θ_{ref} through a low-pass filtering reference model in order to obtain smooth signals. It is therefore not necessary to equip the system with sensors for the absolute velocity, and the knowledge of the relative velocity is sufficient for the implementation.

4.2 Implementation of the control system

The integral LOS control system presented in Section 4.1 was implemented in LabVIEW 2013 analogously to the LOS control system, the implementation details of which have been presented in Section 3.2. In addition to the implementation there, (16) was numerically integrated in LabVIEW in order to account for the effect of the current. The heading controller (14) requires the relative velocity $v_{t,\mathrm{rel}}$ instead of the absolute velocity v_t that was used in Section 3.2. The relative velocity was approximated by subtracting the current speed from the absolute velocity v_t. This way of approximating $v_{t,\mathrm{rel}}$ is only accurate when the robot is heading against the current and will become less accurate when the robot turns. However, this was a

reasonable approximation since the current was mainly opposing the forward motion of the robot, and the calculations were significantly simplified. In order to avoid the singularity in the heading controller and thus achieve a smoother transient in the beginning, the heading controller ϕ_0 was started only after 2 s. The control gains of the system can be found in Table 2. Since a lower bound on the velocity of the

Table 2 The control gains of the integral LOS path-following control system

	α	$g(i)$	ω	δ	k_θ	λ_1	λ_2	Δ	σ
Lateral undulation	30°	1	110°	40°	0.8	0.5	0.2	2 m	0.5
Eel-like motion	50°	$\frac{N-i}{N+1}$	130°	40°	0.9	0.5	0.2	2 m	0.3

robot was not known a priori, it was not feasible to use the theoretical condition (18) to determine a value for σ, and consequently (17) could not be employed to find a bound on Δ. In this light, and following the same line of thoughts as when choosing the look-ahead distance Δ for the classical LOS system in Section 3.2, we made sure to choose a sufficiently large Δ, and a sufficiently small σ in order to converge to the path.

4.3 Experimental validation of the control system

The experimental tests of the integral LOS control system were performed in the North Sea Centre Flume Tank [20] operated by SINTEF Fisheries and Aquaculture in Hirtshals, Denmark. The flume tank is 30 m long, 8 m wide, and 6 m deep and is equipped with four propellers that can generate a circulating flow of up to 1 m/s. For our tests, nine cameras of the Qualisys motion capture system were mounted on one end of the tank. During the experiments, the global coordinate frame was rotated by 45° with respect to the basin, such that the generated current, which is aligned with the long side of the tank, had both an x and a y component. The coordinate transformation is sketched in Figure 8. The snake robot Mamba that was introduced in Section 3.2 served as the test platform also for these experiments. The control system from Section 4.1 was tested experimentally in four different scenarios. In the first two scenarios, the robot was moving with the gait lateral undulation and was exposed to a constant current of $V_c = 0.07$ m/s. In the first case, it was initially headed towards the path, in the second it was initially headed approximately parallel to the path. Similarly, in the third and fourth scenario, the robot was initially headed towards the path and approximately parallel to the path respectively, and propelled with eel-like motion against a current of $V_c = 0.05$ m/s. In all cases, the robot was initially straightened and kept in a fixed position.

The results of the four different test scenarios are presented in Figures 9, 10, 11, and 12. The path of the CM of the robot is presented in Figures 9(a), 10(a), 11(a), and 12(a), respectively. In the first and fourth scenario, there was a small overshoot,

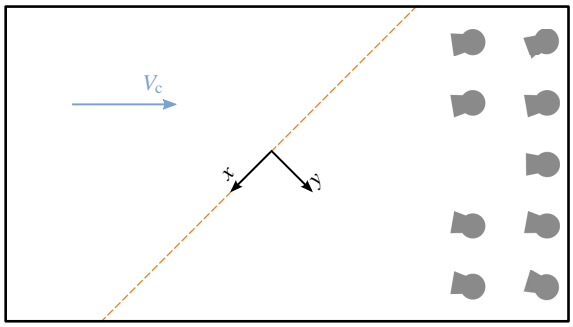

Fig. 8 The coordinate transformation: the global coordinate frame is rotated by 45° with respect to the walls of the tank, such that the current has a negative x-component and a positive y-component. The cameras of the motion capture system (displayed in grey) are mounted on one end of the tank. The path is indicated in orange.

but nevertheless, the robot approached the path and stayed on it in all four scenarios. Just like for the examples in Section 3.3, the CM did not stay constantly on the path after convergence, but oscillated about it. This was expected, since the oscillations of the CM are a consequence of the sinusoidal gait and merely not captured by the simplifications in the control-oriented model. The same effect can also be observed for the heading of the robot, $\bar{\theta}$, that is plotted in Figures 9(b), 10(b), 11(b), and 12(b). The small overshoots in the first and fourth scenario can also be seen in these plots. Unlike in Section 3.3 where the robot was more or less aligned with the path after convergence, the reference signal θ_{ref} instead oscillated about the steady state angle θ^{eq}. This allowed the robot to side-slip along the path and thus compensate for the sideways component of the current. The oscillating nature of the reference signal θ_{ref} is again a result of the oscillations of the CM. The steady-state crab angle θ^{eq} that is depicted in Figures 9(b), 10(b), 11(b), and 12(b) was determined from (19) a posteriori. To this end, we needed the current component V_y and the relative velocity $v_{t,\text{rel}}$. The current component V_y was directly calculated as $V_y = V_c \cos(45°)$ since both the direction and magnitude V_c of the current were known, and the relative velocity $v_{t,\text{rel}}$ was approximated by the average speed $\bar{v}_{\text{rel}}$. The average speed $\bar{v}_{\text{rel}}$ was calculated from the norm of the relative velocity, and the relative velocity components in x and y were obtained by subtracting the current components V_x and V_y from the velocity components of the CM, $\dot{p}_x$ and $\dot{p}_y$. These had been extracted from the position measurements that were obtained during the experiments by using finite differences with a time step of 0.2 s. In order to calculate the average speed for lateral undulation, the measurements of the first scenario were evaluated, and for the average speed for eel-like motion, those of the third scenario were used. It can be seen from the figures that the theoretical result (19) predicted θ^{eq} correctly. The control input for the turning motion, ϕ_0, is shown in Figures 9(c), 10(c), 11(c), and 12(c), respectively. Compared to the tests in Section 3.3, the heading controller was started later, and thus the saturation of ϕ_0 was prevented. After convergence of the robot, ϕ_0 was oscillating about zero, because the robot stayed approximately at the constant angle θ^{eq}. The reference signal and the measured signal of joint number four are displayed in Figures 9(d), 10(d), 11(d), and 12(d). The measured joint angle

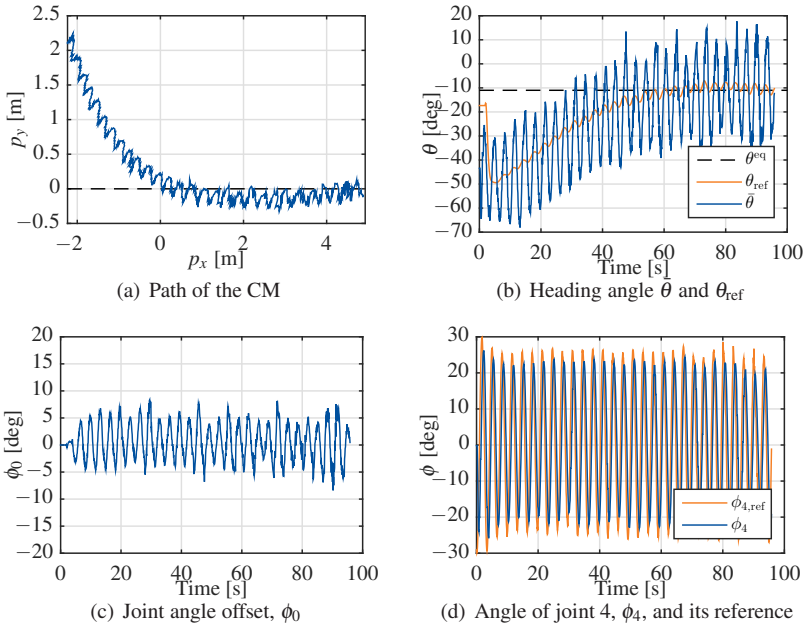

(a) Path of the CM (b) Heading angle $\bar{\theta}$ and θ_{ref}

(c) Joint angle offset, ϕ_0 (d) Angle of joint 4, ϕ_4, and its reference

Fig. 9 Experimental results of the first scenario: Model-based integral LOS path-following with a flow speed $V_c = 0.07$ m/s, lateral undulation and the robot initially headed towards the path.

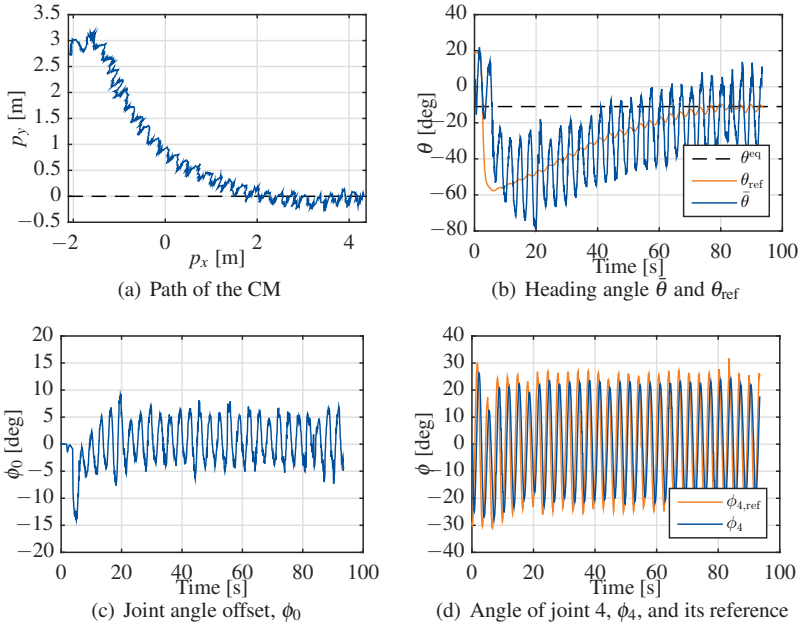

(a) Path of the CM (b) Heading angle $\bar{\theta}$ and θ_{ref}

(c) Joint angle offset, ϕ_0 (d) Angle of joint 4, ϕ_4, and its reference

Fig. 10 Experimental results of the second scenario: Model-based integral LOS path-following with a flow speed $V_c = 0.07$ m/s, lateral undulation and the robot initially headed parallel to the path.

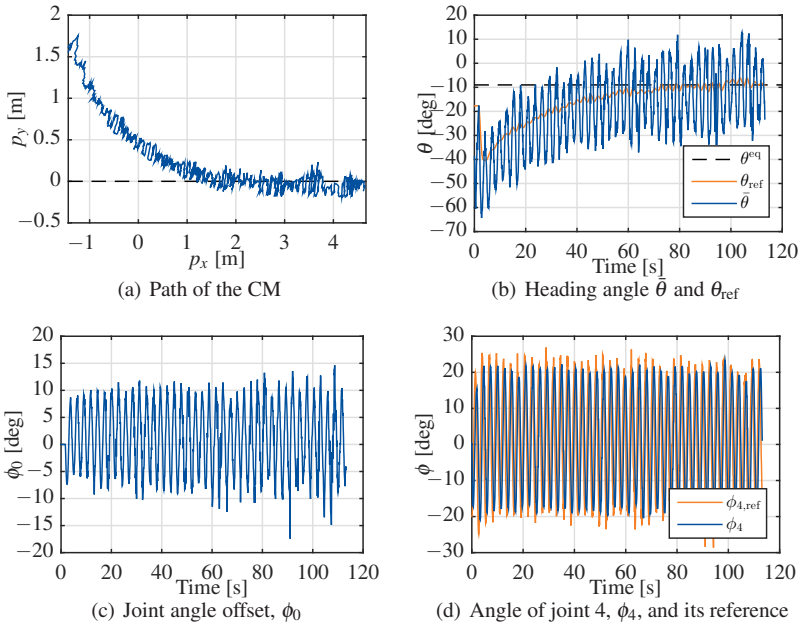

(a) Path of the CM (b) Heading angle $\bar{\theta}$ and θ_{ref}

(c) Joint angle offset, ϕ_0 (d) Angle of joint 4, ϕ_4, and its reference

Fig. 11 Experimental results of the third scenario: Model-based integral LOS path-following with a flow speed $V_{\text{c}} = 0.05$ m/s, eel-like motion and the robot initially headed towards the path.

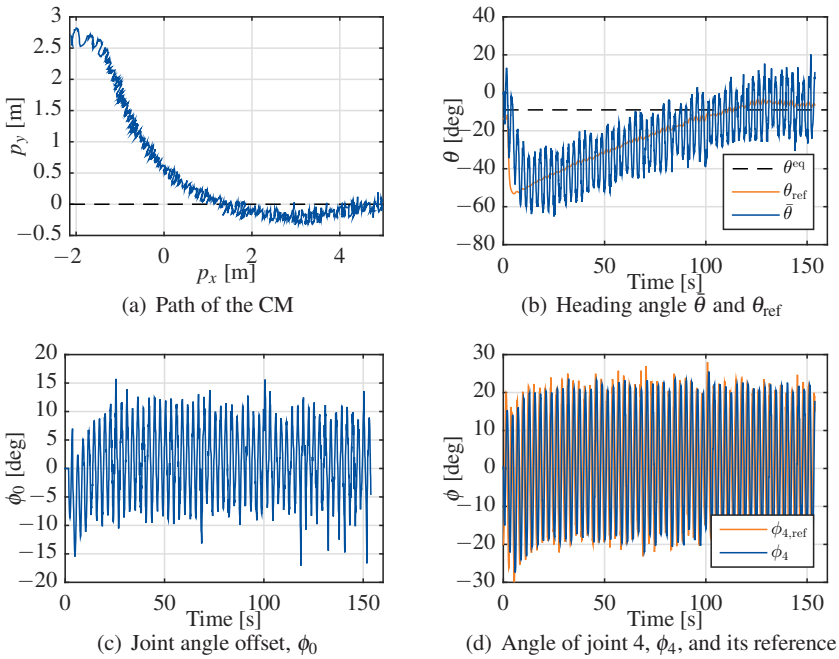

(a) Path of the CM (b) Heading angle $\bar{\theta}$ and θ_{ref}

(c) Joint angle offset, ϕ_0 (d) Angle of joint 4, ϕ_4, and its reference

Fig. 12 Experimental results of the fourth scenario: Model-based integral LOS path-following with a flow speed $V_{\text{c}} = 0.05$ m/s, eel-like motion and the robot initially headed parallel to the path.

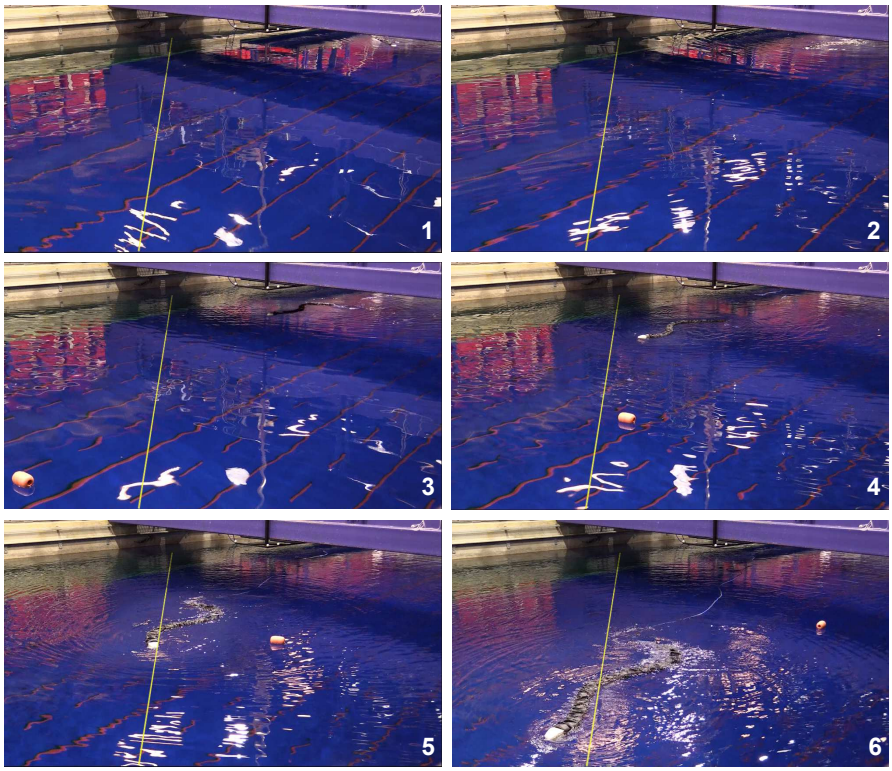

Fig. 13 The snake robot Mamba during a test run of scenario two. The yellow line indicates the path and the buoy visualizes the current effect. The robot is initially approximately parallel to the path (1), turns towards it (2), approaches the path (3) and (4) and subsequently follows it (5) while side-slipping (6).

clearly also tracked its reference. Pictures of the physical robot during the second scenario are presented in Figure 13.

The experimental results validate the model-based integral LOS path-following controller in the presence of constant irrotational currents. The steady-state crab angle θ^{eq} was predicted correctly by the analytical relation in (19). The control objectives (9),(10) are satisfied in the sense that the robot oscillates about the desired values after convergence. As already pointed out in Section 4.3, these oscillations are a result of the sinusoidal motion that the robot conducts and that are not captured by the model in Section 2 that was used for the control design. It was therefore not expected from the theory that these oscillations would be suppressed by the model-based path-following controller.

5 Conclusions

This chapter reviewed and validated a model-based control system for straight line path-following of neutrally buoyant underwater snake robots that move with a planar sinusoidal gait in the presence of unknown, constant, and irrotational ocean currents. The control design was based on a simplified control-oriented snake robot model, which disregards the rotational motion of the single links but captures the overall behaviour of the system. The guidance method that was used in the path-following control system was a LOS guidance scheme, which was augmented with integral action in the presence of currents in order to eliminate the steady state error that the original LOS guidance would give. This was achieved by allowing the robot to head towards a look-ahead point upstream of the path and thus travel at a non-zero crab angle. Experimental results were presented that verify the concept of the control system. Furthermore, the experimental results showed that the crab angle was correctly predicted by the theoretical analysis. Future work will focus on extending the control approach to a three-dimensional control strategy for underwater snake robots.

Acknowledgements The authors gratefully acknowledge the engineers at the Department of Engineering Cybernetics, Glenn Angell and Daniel Bogen for the technical support before and during the experimental tests, Stefano Bertelli and Terje Haugen for preparing the necessary components for the experimental setup, the team at the SINTEF Fisheries and Aquaculture flume tank, Kurt Hansen, Nina A. H. Madsen, and Anders Nielsen for the support during the tests there and Martin Holmberg from Qualisys for setting up the motion capture system.

This work was supported by the Research Council of Norway through its Centres of Excellence funding scheme, project no. 223254-NTNU AMOS, and by VISTA - a basic research program in collaboration between The Norwegian Academy of Science and Letters, and Statoil.

References

1. Børhaug E, Pavlov A, Pettersen K Y (2008) Integral LOS control for path following of underactuated marine surface vessels in the presence of constant ocean currents. Proceedings of the 47th IEEE Conference on Decision and Control, Cancun, Mexico 4984–4991
2. Colgate J E, Lynch K M (2004) Mechanics and control of swimming: A review. IEEE Journal of Oceanic Engineering 29(3):660–673
3. Fossen T I (2001) Handbook of Marine Craft Hydrodynamics and Motion Control. Wiley
4. Guo J (2006) A waypoint-tracking controller for a biomimetic autonomous underwater vehicle. Ocean Engineering 33:2369–2380
5. Hirose S (1993) Biologically Inspired Robots: Snake-Like Locomotors and Manipulators. Oxford University Press
6. Hopkins J K, Spranklin B W, Gupta S K (2009) A survey of snake-inspired robot designs. Bioinspiration & Biomimetics (4) 021001
7. Kelasidi E, Liljebäck P, Pettersen K Y, Gravdahl J T (2016) Innovation in Underwater Robots: Biologically Inspired Swimming Snake Robots. IEEE Robotics and Automation Magazine 23(1):44–62

8. Kelasidi E, Liljebäck P, Pettersen K Y, Gravdahl J T (2016) Integral Line-of-Sight Guidance for Path Following Control of Underwater Snake Robots: Theory and Experiments. IEEE Transactions on Robotics (conditionally accepted)
9. Kohl A M, Pettersen K Y, Kelasidi E, Gravdahl J T (2015) Analysis of underwater snake robot locomotion based on a control-oriented model. Proceedings of the IEEE International Conference on Robotics and Biomimetics, Zhuhai, China 1930–1937
10. Kohl A M, Kelasidi E, Mohammadi A et al (2016) Planar maneuvering control of underwater snake robots using virtual holonomic constraints. Bioinspiration & Biomimetics (accepted)
11. Kohl A M, Pettersen K Y, Kelasidi E, Gravdahl J T (2016) Planar path following of underwater snake robots in the presence of ocean currents. IEEE Robotics and Automation Letters 1(1):383–390
12. Kruusmaa M, Fiorini P, Megill W et al (2014) FILOSE for Svenning: A Flow Sensing Bioinspired Robot. IEEE Robotics and Automation Magazine 21(3):51–62
13. Liljebäck P, Pettersen K Y, Stavdahl Ø, Gravdahl J T (2012) Snake Robots: Modelling, Mechatronics, and Control. Springer London
14. Liljebäck P, Pettersen K Y, Stavdahl Ø, Gravdahl J T (2012) A review on modelling, implementation, and control of snake robots. Robotics and Autonomous Systems 60:29–40
15. Liljebäck P, Stavdahl Ø, Pettersen K Y, Gravdahl J T (2014) Mamba – A waterproof snake robot with tactile sensing. Proceedings of the IEEE/RSJ International Conference on Intelligent Robots and Systems, Chicago, IL, USA 294–301
16. Mohammadi A, Rezapour E, Maggiore M, Pettersen K Y (2015) Maneuvering Control of Planar Snake Robots Using Virtual Holonomic Constraints. IEEE Transactions on Control Systems Technology 24(3):884–899
17. Marine cybernetics laboratory (MC-lab) – operated by the Department of Marine Technology, Trondheim, Norway.
18. McIsaac K, Ostrowski, J (2003) Motion Planning for Anguilliform Locomotion. IEEE Transactions on Robotics and Automation 19(4):637–652
19. Raj A, Thakur A (2009) Fish-inspired robots: design, sensing, actuation, and autonomy – a review of research. Bioinspiration & Biomimetics (11) 031001
20. The North Sea Centre Flume Tank – Managed and operated by SINTEF Fisheries and Aquaculture, Hirtshals, Denmark.
21. Qualisys – Motion Capture Systems.